CACNB1 alleviates mepivacaine-induced myocardial ischemia/reperfusion injury by promoting Nrf2 nuclear translocation

QINGBO SHAO*, JI ZHANG* and HUAYING WANG

Department of Anesthesiology, Minhang Hospital, Fudan University, Shanghai 201199, P.R. China

Received January 9, 2025; Accepted September 2, 2025

DOI: 10.3892/mmr.2025.13781

Abstract. Myocardial ischemia/reperfusion injury (MIRI) is a challenging cardiovascular disease. Mepivacaine, a common local anesthetic, exacerbates myocardial injury during ischemia-reperfusion (IR). Understanding the underlying mechanisms of MIRI and potential therapeutic targets is important to treat this disease. In the present study, differentially expressed genes (DEGs) from the GSE19339 dataset were identified and analyzed. The expression of calcium voltage-gated channel auxiliary subunit β1 (*CACNB1*) was measured in myocardial infarction samples and the effects of different doses of mepivacaine on cell cycle progression, apoptosis, cell viability, inflammatory response and oxidative stress were evaluated in H9c2 cells. Hypoxia-reoxygenation (H/R) treatment simulated MIRI, highlighting the role of *CACNB1* in mepivacaine-induced cellular inflammation and injury. The present study identified 2,396 upregulated and 1,230 downregulated DEGs enriched in pathways such as inflammatory response and chemokine signaling. Mepivacaine induced apoptosis, G_1 phase arrest and increased oxidative stress markers, including elevated ROS and MDA levels together with decreased SOD activity, as well as inflammatory cytokines (TNF-α, IL-1β and IL-6), in a dose-dependent manner in H9c2 cells. *CACNB1* knockdown reduced mepivacaine- and H/R-induced damage, inhibiting inflammation and apoptosis via the CACNB1/NOD-like receptor protein 3 (NLRP3)/Nuclear factor erythroid 2-related factor 2 (Nrf2) axis. Furthermore, *CACNB1* knockdown enhanced Nrf2 nuclear translocation, indicating a stress response mechanism. Mepivacaine exacerbated MIRI by inducing apoptosis, G_1 phase arrest, oxidative stress and inflammation in H9c2 cells. *CACNB1* knockdown reduced these effects. Targeting the CACNB1/NLRP3/Nrf2 axis may be a potential strategy for mitigating myocardial injury caused by mepivacaine and IR.

Correspondence to: Dr Huaying Wang, Department of Anesthesiology, Minhang Hospital, Fudan University, 170 Xinsong Road, Minhang, Shanghai 201199, P.R. China
E-mail: 18918166933@163.com

*Contributed equally

Key words: myocardial ischemia/reperfusion injury, mepivacaine, calcium voltage-gated channel auxiliary subunit β 1, nuclear factor erythroid 2-related factor 2, nuclear translocation

Introduction

Myocardial infarction (MI), a critical condition among cardiovascular diseases, is primarily caused by inadequate blood supply to the myocardium, resulting in ischemia and subsequent necrosis (1). This pathology is markedly influenced by numerous risk factors, including obesity, smoking, hypertension, hypercholesterolemia and poor dietary habits (2). Clinically, MI is typically manifested through chest pain, along with symptoms such as chest tightness, dyspnoea, nausea and vomiting (3). The incidence of MI varies regionally and by population, typically ranging from a few hundred to several thousand cases per 100,000 individuals per year (4,5). The mortality associated with MI is influenced by several factors, including age, sex, preexisting cardiac health and the quality of care received (6). Timely and effective interventions, including emergency resuscitation, anticoagulant and antiplatelet therapies, vasodilators or coronary artery bypass grafting (CABG), are key and have been revealed to reduce notably mortality (7). In addition, a previous study suggested that the use of volatile anaesthetics during CABG may reduce postoperative MI rates and long-term cardiac mortality (8).

Mepivacaine, a local anesthetic, is commonly used to reduce pain during various medical procedures through the inhibition of sodium channels in nerve cells (9). This function hinders the transmission of nerve impulses, thereby facilitating local anaesthesia. Although considered relatively safe, mepivacaine can cause side effects such as overdose, allergic reactions and nerve damage (10). A protocol study by Dell'Olio *et al* (11) suggested that light-conscious sedation with mepivacaine may effectively manage postoperative pain in patients with acute MI (AMI). Further experimental evidence revealed that mepivacaine markedly reduces calcium transients in adult mouse cardiomyocytes (12). This is achieved through sodium channel blockade and enhancement of the reverse mode activity of the sodium-calcium exchanger, suggesting a novel mechanism by which mepivacaine may reduce myocardial contractility. In addition, a clinical case report by de Groot-van der Mooren *et al* (13)

described an infant with unexplained cardiorespiratory distress and neurological symptoms shortly after birth, possibly related to maternal exposure to mepivacaine. This case study raised concerns regarding the possible function of mepivacaine in the emergence of cardiovascular and neurological adverse effects.

The calcium voltage-gated channel auxiliary subunit β1 (*CACNB1*) gene, located on chromosome 12 of the human genome, encodes the β1 subunit of the voltage-gated calcium channel (14). In cardiomyocytes, voltage-gated calcium channels are essential for controlling cardiac muscle contraction (15). The β subunit encoded by the *CACNB1* gene forms a complex with the α1 subunit in cardiomyocytes, contributing to the functionality of the calcium channel complex (16). Abnormalities in this function of the complex may affect calcium channel activity, thereby influencing cardiomyocyte excitability and contractility. Previous studies have reported that abnormal expression of *CACNB1* in cardiac muscle cells is associated with such as arrhythmias, myocardial hypertrophy and heart failure (17,18). A study revealed that the *CACNB1* gene encodes the CaVβ1 protein, which regulates T-cell function (17). After infection with the lymphocytic choriomeningitis virus, deletion of *CACNB1* increased T-cell death and inhibited clonal proliferation. However, *CACNB1* is not necessary for T-cell proliferation, cytokine production or Ca^{2+} signal transduction. Xuan *et al* (18) demonstrated that the levels of potassium voltage-gated channel subfamily D member 3 (KCND3), CACNB1 and potassium inwardly rectifying channel subfamily J member 2 (*KCNJ2*) proteins can be regulated by microRNA 195 through direct interactions with *KCND3*, *CACNB1* and *KCNJ2* genes. Therefore, further exploration of the potential role of *CACNB1* in MI is warranted.

In the context of MI, understanding the molecular mechanisms of cardiomyocyte injury is key for developing effective treatment plans. The present study aimed to elucidate the impacts of mepivacaine on apoptosis, cell viability, cell cycle regulation, inflammatory responses and oxidative stress in H9c2 cells. Furthermore, through *CACNB1* knockdown experiments, the protective effect of *CACNB1* against mepivacaine- and hypoxia/reoxygenation (H/R)-induced injury was investigated, highlighting its potential as a therapeutic target to attenuate myocardial injury. The present study reveals an innovative view into the pathogenic processes and therapeutic interventions of mepivacaine in the context of MI.

Materials and methods

Differential expression analysis of the GSE19339 dataset. The GSE19339 dataset, available in the Gene Expression Omnibus database (https://www.ncbi.nlm.nih.gov/gds/), was used to identify genes associated with MI. This data set comprises transcriptomic data from four patients with MI and four normal individuals. The 'limma' package in the R programming language (version 3.5.3; http://www.r-project.org/) was used to carry out the differential expression analysis. The fold change (FC) criterion was employed to assess differentially expressed genes (DEGs), with FC ≤0.77 designating downregulated DEGs and FC ≥1.3 designating upregulated DEGs. $P<0.05$ was considered to indicate a statistically significant difference.

Functional enrichment analysis of DEGs and expression analysis of CACNB1 in MI. The Database for Annotation, Visualization, and Integrated Discovery (DAVID) (https://david.ncifcrf.gov/tools.jsp) was employed to elucidate the functional characteristics of MI-related DEGs. Analysis also included the Kyoto Encyclopedia of Genes and Genomes (KEGG; http://www.kegg.jp/) pathway and Gene Ontology (GO; http://geneontology.org/) term. GO classification facilitates the categorization of gene and protein functions into three hierarchical classifications: Biological Process (BP), Molecular Function (MF) and Cell Component (CC). Finally, the *CACNB1* gene expression in the MI and normal groups was assessed using the GSE19339 dataset, which was analyzed using the R software (version 3.5.3).

Culturing and maintenance of H9c2 cells. H9c2 cells (cat. no. GNR 5, National Collection of Authenticated Cell Cultures), a rat ventricular cardiomyocyte cell line, were purchased from the Shanghai Institute of Biochemistry and Cell Biology. H9c2 cells were cultured under conventional cell culture conditions, which include a humidified environment at 37˚C with 5% CO_2, using DMEM (cat. no. 10566016; Gibco; Thermo Fisher Scientific, Inc.) supplemented with 10% foetal bovine serum (Gibco; Thermo Fisher Scientific, Inc.). The cell culture solution was refreshed regularly to maintain cell viability and growth. All experiments were carried out using cells within passages 3-5 after cell recovery. The H9c2 cell line was authenticated through short tandem repeat analysis and evaluated for mycoplasma contamination, with negative results.

Cell transfection and treatment. Transfection was carried out on H9c2 cells utilizing the following specific small interfering RNA (siRNA) targeting CACNB1: si-CACNB1-1, sense 5'-CAAGACCAAGCCAGUGGCAUUUGCU-3' and antisense, 5'-AGCAAAUGCCACUGGCUUGGUCUUG-3'; si-CACNB1-2 sense, 5'-CAAUGUCCAAAUAGCGGC CUCGGAA-3' and antisense, 5'-UUCCGAGGCCGCUAU UUGGACAUUG-3'; and negative control siRNA (si-NC), sense 5'-CAAACCUAUAAGGCGCUCCGGUGAA-3' and antisense, 5'-UUCACCGGAGCGCCUUAUAGGUUU G-3'. All siRNAs, including CACNB1-siRNA and negative control siRNA, were purchased from Shanghai GenePharma Co., Ltd. H9c2 cells were transfected with siRNAs (at a final concentration of 50 nM) using Lipofectamine® 2000 (Invitrogen; Thermo Fisher Scientific, Inc.) after being cultured in 24-well plates. Cells were incubated with the transfection mixture at 37˚C in a humidified atmosphere with 5% CO_2 for 6 h, after which the medium was replaced with fresh DMEM supplemented with 10% FBS. All transfections were carried out using the same procedure. At 48 h post-transfection, to explore the impact of mepivacaine on H9c2 cells, the cells were subjected to different mepivacaine concentrations (0.5, 1.0, 2.0, 5.0, 7.0 and 10.0 mM; cat. no. HY-B0517; MedChemExpress; CAS No. 96-88-8) at 37˚C in a humidified atmosphere with 5% CO_2 for 24 h. After mepivacaine treatment, cells were harvested for subsequent analyses.

Cell Counting Kit-8 (CCK-8) assay. A CCK-8 assay (cat. no. CK04; Dojindo Laboratories, Inc.) was employed to

measure cell viability. H9c2 cells were seeded in a 96-well plate at a density of $5x10^3$ cells/well. Subsequently, each well was treated with 10 μl CCK-8 reagent and the wells were then incubated at 37˚C with 5% CO_2 for 4 h. Subsequently, the absorbance at 450 nm was measured utilizing a microplate reader (Thermo Fisher Scientific, Inc.).

Reverse transcription-quantitative PCR (RT-qPCR). H9c2 cells were treated with the TRIzol® Reagent (Invitrogen; Thermo Fisher Scientific, Inc.) to extract total RNA. The purity and concentration of the RNA were evaluated through spectrophotometric analysis. The SuperScript III First-Strand Synthesis System (Invitrogen; Thermo Fisher Scientific, Inc.) was used for the synthesis of complementary DNA, with 1 μg of the extracted RNA being reverse-transcribed. Subsequently, the Applied Biosystems 7500 Fast Real-Time PCR System (Applied Biosystems; Thermo Fisher Scientific, Inc.) was employed to carry out qPCR analysis using the following primer pairs: CACNB1, forward, 5'-AGGGCTATGAGGTAA CTGAC-3' and reverse, 5'-GGAAATCCTGCCATCAAA CC-3'); Bax forward, 5'-TGAAGACAGGGGCCTTTTTG-3' and reverse, 5'-AATTCGCCTGAGACACTCG-3'); Bcl-2 forward, 5'-ATGCCTTTGTGGAACTATATGGC-3' and reverse, 5'-GGTATGCACCCAGAGTGATGC-3'; Caspase-3 forward, 5'-AGCATTTCCCATAAGCCTCCT-3' and reverse, 5'-AGCACCAAAAGTATCATTGGC-3'; P21 forward, 5'-ACC CCAGATAACCAAGGATGC-3' and reverse, 5'-AGAACA CCATCTTGCCCTTGT-3'; Cyclin E1 forward, 5'-GACACA GCTTCGGGTACGG-3' and reverse, 5'-TTGCTGTGGTCC TTCGAGTC-3'; CDK4 forward, 5'-CTTCCCGTCAGCACA GTTC-3' and reverse, 5'-GGTCAGCATTTCCAGCAGC-3'; and GAPDH forward, 5'-ACGGGAAACCCATCACCATC-3' and reverse, 5'-CTCGTGGTTCACACCCATCA-3'. GAPDH was used as an internal reference. The thermocycling conditions were as follows: Initial denaturation at 95˚C for 10 min, followed by 40 cycles of denaturation at 95˚C for 15 sec and annealing/extension at 60˚C for 1 min. A melt curve analysis (60-95˚C) was performed to verify amplification specificity. The expression was examined utilizing the $2^{-\Delta\Delta Cq}$ method (19).

Western blotting (WB). Total protein lysates from H9c2 cells were prepared utilizing RIPA lysis buffer (Thermo Fisher Scientific, Inc.) containing protease and phosphatase inhibitors (Thermo Fisher Scientific, Inc.). The BCA Protein Assay Kit (Beyotime Institute of Biotechnology) was used to measure the protein content. Equal amounts of protein (30 μg per lane) were separated on 10% gels using SDS-PAGE and then transferred onto PVDF membranes (MilliporeSigma). The membranes were blocked with 5% non-fat milk in TBS-Tween (TBST; 0.1% (v/v) Tween-20) at room temperature for 1 h and then incubated overnight at 4˚C with the following primary antibodies: CACNB1 (1:1,000; cat. no. 13039-1-AP; Proteintech Group, Inc.), Bax (1:20,000; cat. no. 50599-2-Ig; Proteintech Group, Inc.), Caspase-3 (1:1,000; cat. no. 19677-1-AP; Proteintech Group, Inc.), Bcl-2 (1:2,000; cat no. 26593-1-AP; Proteintech Group, Inc.), P21 (1:1,000; cat no. 28248-1-AP; Proteintech Group, Inc.), CDK4 (1:1,000; cat no. 11026-1-AP; Proteintech Group, Inc.), Cyclin E1 (1:1,000; cat no. AF0144; Affinity Biosciences), NOD-like receptor protein 3 (NLRP3; 1:2,000; cat no. 30109-1-AP; Proteintech Group, Inc.), Caspase-1 (1:2,000; cat no. 31020-1-AP; Proteintech Group, Inc.), C-Caspase-1 (1:1,000; cat no. AF4005; Affinity Biosciences), GSDMD (1:2,000; cat no. 20770-1-AP; Proteintech Group, Inc.), IL-18 (1:2,000; cat no. DF6252; Affinity Biosciences), ASC (1:5,000; cat no. 30641-1-AP; Proteintech Group, Inc.), IL-1β (1:2,000; cat no. AF5103; Affinity Biosciences), nuclear factor erythroid 2-related factor 2 (Nrf2; 1:1,000; cat no. AF0639; Affinity Biosciences), GAPDH (1:5,000; cat no. 10494-1-AP; Proteintech Group, Inc.) and Lamin B (1:2,000, cat no. 12987-1-AP; Proteintech Group, Inc.). After secondary antibody incubation with HRP-conjugated goat anti-rabbit IgG (1:5,000; cat. no. SA00001-2; Proteintech Group, Inc.) at room temperature for 1 h, bands were developed using an ECL kit (Cytiva) and captured on ImageJ software (version 1.8.0; National Institutes of Health).

Flow cytometry analysis. Flow cytometry analysis was carried out to evaluate apoptosis in H9c2 cells. After being seeded in 24-well plates at a density of $1x10^4$ cells/well, H9c2 cells were grown for 24 h at 37˚C in a humidified 5% CO_2 incubator. Following cell detachment with trypsin-EDTA (0.25% trypsin and 0.02% EDTA), the cells were collected by centrifugation at 300 x g for 5 min at 4˚C, washed twice with PBS, and resuspended. Subsequently, the cells were cultured with 5 μl Annexin V-fluorescein isothiocyanate and 5 μl of PI solution at ambient temperature for 15 min for apoptosis analysis. The staining with PI and Annexin V was then evaluated using a flow cytometer (CyFlow® Cube 6; Sysmex-Partec; Guangzhou Jiyuan Biotechnology Co., Ltd.) and the FlowJo program (version 7.4.1; BD Biosciences) was employed to analyze the data.

Measurement of oxidative stress biomarkers in H9c2 cells. H9c2 cells were plated in 96-well plates at a density of $1x10^4$ cells/well and allowed to adhere for 24 h at 37˚C in a humidified incubator with 5% CO_2. After adhesion, the cells were rinsed twice with PBS and then lysed. The supernatants were separated from the lysates through centrifugation at 10,000 x g for 5 min at 4˚C. To aid homogeneity, the supernatants were sonicated on ice at 20 kHz for 3x10 sec bursts with 10 sec intervals. The prepared samples were utilized to measure the expression of lactate dehydrogenase (LDH) activity, reactive oxygen species (ROS), superoxide dismutase (SOD) activity and malondialdehyde (MDA) content. The assays for SOD and MDA were conducted utilizing commercial kits (Nanjing Jiancheng Bioengineering Institute). The ROS assay and LDH activity were evaluated utilizing a kit from Beyotime Institute of Biotechnology. All measurements were carried out in triplicate and the data were standardized to protein content in the samples to account for variations in cell density across wells.

ELISA. In the present study, the secretion of IL-1β, TNF-α and IL-8 in the culture supernatants of H9c2 cells, either untreated or treated with mepivacaine (0.5, 1 and 2 mM for 24 h), was determined using ELISA kits for IL-1β (cat. no. CSB-E08055r; Cusabio Technology, LLC), TNF-α (cat. no. CSB-E11987r; Cusabio Technology, LLC), and IL-8 (cat. no. SEKR-0014; Beijing Solarbio Science & Technology Co., Ltd.). The absorbance at 450 nm was measured using an ELISA reader.

The obtained values were compared with standard curves established using standard titration. The BCA test was utilized to ascertain the protein content in each culture bottle. All concentrations were standardized to the respective cellular protein content and expressed as pg/ml (cellular protein).

H/R model and treatment in H9c2 cells. After being moved to the cell culture equipment, H9c2 cells were treated with a hypoxic buffer solution (1% O_2 + 5% CO_2 + 94% N_2) to exhaust any remaining oxygen for 2 h at 37˚C. Cells were then exposed to 3 h of hypoxia in a constant temperature CO_2 incubator at 37˚C with 95% humidity. After hypoxic exposure, the cells were reoxygenated under normal oxygen conditions (21% O_2, 74% N_2 and 5% CO_2) at 37˚C for 2 h following the replacement of the buffer solution with a standard culture medium. Cell samples were randomly divided into three groups: i) Control, with normal incubation (37˚C, 5% CO_2, 95% humidity) for 6 h; ii) HR, pre-treated with 2 mM mepivacaine for 24 h before H/R induction, followed by 2 h of reoxygenation after 3 h of hypoxia; iii) si-*CACNB1*-1 + HR, pre-treated with 2 mM mepivacaine for 24 h before H/R induction and then transfected with *CACNB1-1* siRNA, as described in the *'Cell transfection and treatment'* section.

Statistical analysis. R software was employed for statistical analysis of the current dataset. The normality of data distribution was assessed using the Shapiro-Wilk normality test. $P>0.05$ indicated that the data were normally distributed. Comparisons between two independent groups of normally distributed data were analyzed using an unpaired, two-tailed Student's t-test. For comparisons involving more than two groups, a one-way ANOVA followed by Tukey's post-hoc test was applied to control the familywise error rate. All quantitative data are presented as mean ± standard deviation. $P<0.05$ was considered to indicate a statistically significant difference. To ensure equal protein loading in western blot analyses, GAPDH was used as the loading control for cytoplasmic proteins, while Lamin B was used for nuclear proteins. In the RT-qPCR analyses, GAPDH was used as the internal reference. Each experiment was independently repeated at least three times with separate biological samples to ensure reproducibility and reliability of statistical analysis.

Results

Functional enrichment analysis of GSE19339-DEGs and expression verification of CACNB1. DEG analysis was carried out on samples from the GSE19339 dataset using the 'limma' package, resulting in the identification of 2,396 upregulated DEGs and 1,230 downregulated DEGs (Fig. 1A). Subsequently, functional enrichment analysis was conducted on the DEGs. Analysis of GO terms revealed significant enrichment of DEGs in BP such as 'Chemokine-Mediated Signalling Pathway', 'Inflammatory Response' and 'Regulation Of Cell Migration' (Fig. 1B). Moreover, in CC terms, DEGs demonstrated notable enrichment in 'Endoplasmic Reticulum Lumen', 'Adherens Junction' and 'Actin Cytoskeleton' (Fig. 1C). For MF terms, DEGs exhibited significant enrichment in 'Protein Kinase Binding', 'Protein Tyrosine Kinase Activity' and 'Cadherin Binding' (Fig. 1D). As depicted in Fig. 1E, in the KEGG pathways, the majority of DEGs were enriched in pathways such as 'PI3K-Akt signalling pathway', 'Fluid shear stress and atherosclerosis' and 'Proteoglycans in cancer'. Given that *CACNB1* has been previously associated with cardiovascular diseases (20,21) and encodes the β1 subunit of the voltage-gated calcium channel, which is essential for regulating calcium influx and modulating cardiac muscle contraction, *CACNB1* was selected as the target gene. Further investigation revealed that the expression of *CACNB1* was upregulated in MI samples of the GSE19339 dataset, suggesting a potential role of this gene in enhancing cardiac dysfunction or exacerbating disease pathology in MI (Fig. 1F).

Mepivacaine induces apoptosis in H9c2 cells in a dose-dependent manner. Clinically relevant plasma concentrations of mepivacaine may vary depending on the specific application and patient population. For example, in a study on plasma mepivacaine concentrations in patients undergoing anesthesia, the peak plasma concentration ranged from 0.77-8.31 μg/ml (22). Based on preliminary experiments (Fig. S1), the concentrations of 0.5, 1.0 and 2.0 mM for mepivacaine were used (23). Cell viability and apoptosis in H9c2 cells subjected to different concentrations (0.5, 1.0 and 2.0 mM) of mepivacaine were assessed using flow cytometry, as well as CCK-8 assays (Fig. 2A and B). The outcomes demonstrated that there was a dose-dependent reduction in cell viability of H9c2 cells with increasing concentrations of mepivacaine, while the apoptosis rate increased. Subsequent analysis using RT-qPCR examined the effects of mepivacaine treatment on apoptotic factors (caspase-3, Bax and Bcl-2) in H9c2 cells (Fig. 2C-E). Compared with the control group, levels of Caspase-3 and Bax increased, whereas the expression of Bcl-2 decreased with increasing concentrations of mepivacaine. These changes were further confirmed through semi-quantification of protein expression (Fig. 2F-I). Collectively, these findings suggested that mepivacaine induces apoptosis in H9c2 cells in a concentration-dependent manner.

Mepivacaine modulates cell cycle regulatory factors to induce G_1 arrest in H9c2 cells. The influence of mepivacaine on cell cycle dynamics in H9c2 cells was investigated by assessing the expression of key cell cycle regulators, including Cyclin E1, P21 and CDK4. RT-qPCR and WB analysis were utilized to measure changes in the levels of cell cycle regulators after exposure to varying concentrations of mepivacaine (0.5, 1.0 and 2.0 mM; Fig. 3A-G). The data revealed a dose-dependent increase in P21 expression, with significant elevations at 1 and 2 mM mepivacaine, suggesting an enhanced inhibitory effect on the cell cycle (Fig. 3A and E). Conversely, the levels of CDK4 and Cyclin E1, key promoters of the G_1 to S phase transition, revealed a marked decrease across the same mepivacaine concentrations (Fig. 3B, C, F and G). This reciprocal regulation of cell cycle proteins suggested that mepivacaine induces G_1 phase arrest in H9c2 cells by disrupting the balance of cell cycle regulators required for progression into the S phase.

Mepivacaine induces oxidative stress and inflammation in H9c2 cells. To explore the impact of mepivacaine on oxidative

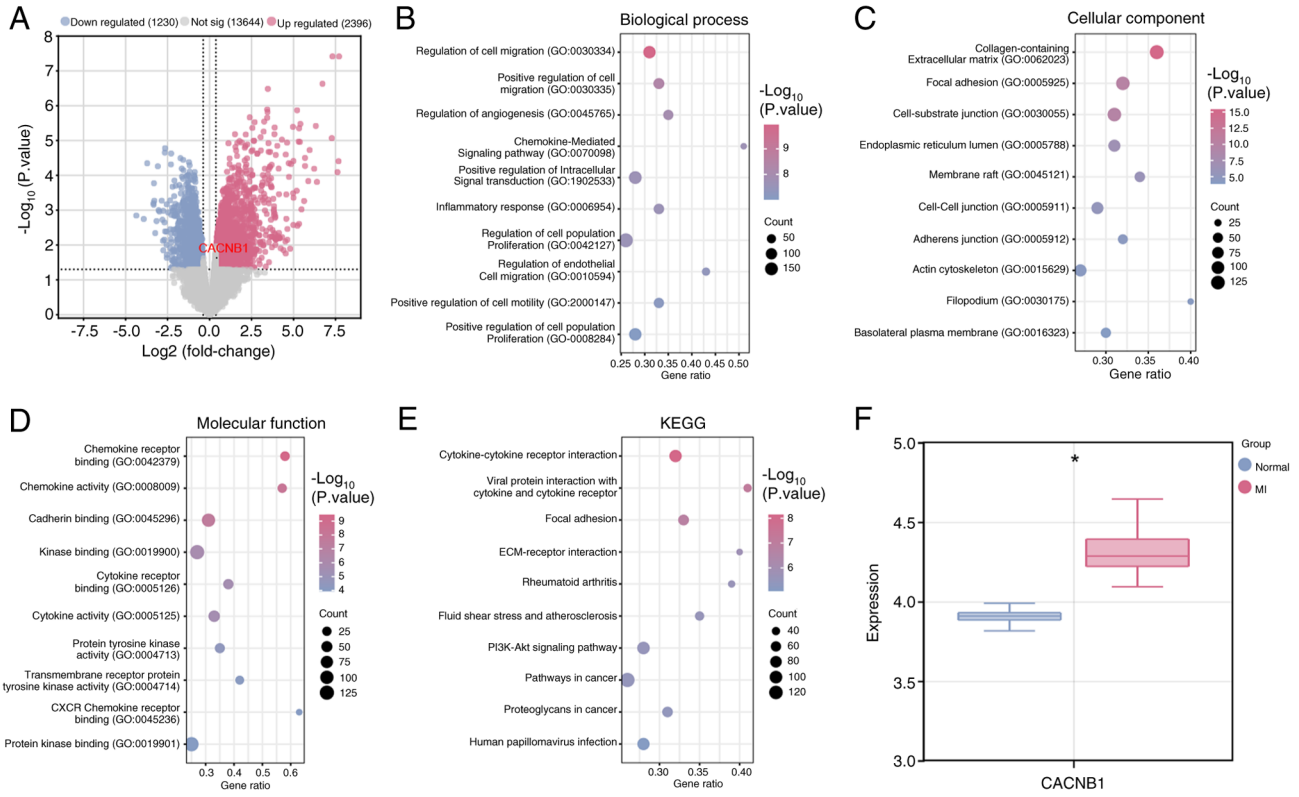

Figure 1. Differential expression and functional enrichment analyses for hub gene identification in the GSE19339 dataset. (A) Volcano plot displaying the differential expression analysis results of the GSE19339 dataset. The x-axis represents the $\log_2$ fold change in gene expression between MI and normal samples. The y-axis indicates the statistical significance of differential expression. Upregulated DEGs are depicted in red, and downregulated DEGs are depicted in blue. Gene ontology enrichment analysis of the function of DEGs based on (B) biological process, (C) cellular component and (D) molecular function. The abscissa is GeneRatio and the ordinate is an enrichment term. The larger the dots, the more genes that are enriched. (E) KEGG enrichment analysis predicted the pathways of overlapping gene involvement. (F) Box plot showing the differential expression of *CACNB1* between MI and normal samples in the GSE19339 dataset, $^*P<0.05$ compared with the Normal group. Statistical analysis of differential gene expression was performed using an unpaired Student's t-test. DEGs, differentially expressed genes; KEGG, Kyoto Encyclopedia of Genes and Genomes; MI, myocardial infarction.

stress in H9c2 cells, the expression levels of ROS, SOD, MDA and LDH were assessed using the corresponding assay kits after exposure to varying concentrations of mepivacaine (Fig. 4A-D). The outcomes indicated that compared with the control group, the ROS, MDA and LDH levels increased with increasing concentrations of mepivacaine, while SOD levels decreased. These findings suggested that mepivacaine induces oxidative stress and cell damage in H9c2 cells. Subsequently, the secretion levels of inflammatory cytokines (IL-1β, TNF-α and IL-8) in H9c2 cells after exposure to different concentrations of mepivacaine were measured using ELISA experiments (Fig. 4E-G). The current findings demonstrated that, compared with the control group, the expression levels of IL-1β, TNF-α and IL-8 increased with increasing concentrations of mepivacaine. This indicated a significant pro-inflammatory effect of mepivacaine in H9c2 cells.

CACNB1 knockdown protects H9c2 cells from mepivacaine and H/R-induced injury. The effect of mepivacaine treatment at several concentrations on the expression of *CACNB1* in H9c2 cells was investigated using RT-qPCR and WB analyses (Fig. 5A-C). Analysis revealed that as the mepivacaine concentration increases, the level of *CACNB1* in H9c2 cells also increases. Furthermore, *CACNB1* expression was highest under treatment with 2 mM mepivacaine; therefore, this particular concentration was used for further experiments. Subsequently, the transfection efficiency of *CACNB1* knockdown plasmids was assessed with RT-qPCR and WB analyses, with si-*CACNB1*-1 demonstrating the greatest efficacy. Therefore, si-*CACNB1*-1 was used for knockdown experiments (Fig. 5D-F). The viability of H/R model H9c2 cells subjected to 2 mM mepivacaine for 24 h, combined with *CACNB1* knockdown, was assessed with the CCK-8 assay (Fig. 5G). The findings indicated that the viability of H/R-treated cells was notably reduced compared with the control group, whereas knockdown of *CACNB1* significantly improved cell viability compared with the H/R group. This suggested that *CACNB1* knockdown protects cardiomyocytes from injury induced by mepivacaine and H/R.

CACNB1 knockdown attenuates apoptosis in H/R model H9c2 cells treated with mepivacaine. Flow cytometry was used to measure the level of apoptosis in H/R model H9c2 cells subjected to 2 mM mepivacaine in combination with *CACNB1* knockdown (Fig. 6A). The results indicated a notable increase in the apoptosis rate in the H/R group in comparison with the control group, while the apoptosis rate was decreased in the H/R group with *CACNB1* knockdown compared with the H/R group. Subsequently, RT-qPCR and WB analyses were conducted

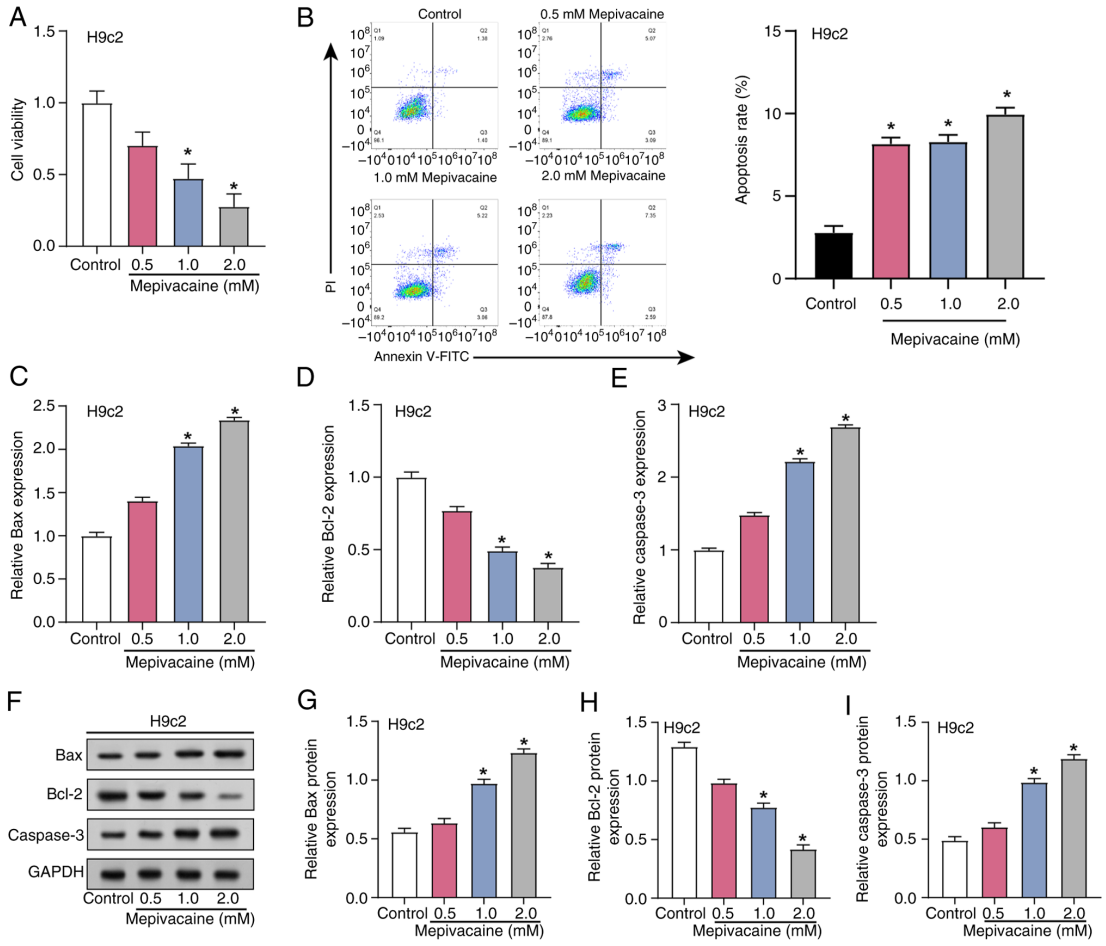

Figure 2. Mepivacaine induces activation of the apoptosis pathway in H9c2 cells. (A) Determination of cell viability in H9c2 cells treated with different concentrations (0.5, 1.0 and 2.0 mM) of mepivacaine using the CCK-8 assay. The x-axis represents different treatment conditions and the y-axis represents cell viability. (B) Analysis of apoptosis rate in H9c2 cells treated with different concentrations (0.5, 1.0 and 2.0 mM) of mepivacaine using flow cytometry. Reverse transcription-quantitative pcr analysis of mRNA expression levels of apoptotic factors (C) Bax, (D) Bcl-2 and (E) Caspase-3 in H9c2 cells treated with different concentrations of mepivacaine. (F) Representative images of western blot analysis of protein expression levels of (G) Bax, (H) Bcl-2 (I) and Caspase-3 in H9c2 cells treated with different concentrations of mepivacaine. Data are presented as mean ± SD. Statistical significance was assessed using one-way ANOVA followed by Tukey's post hoc test. *P<0.05 compared with the Control group.

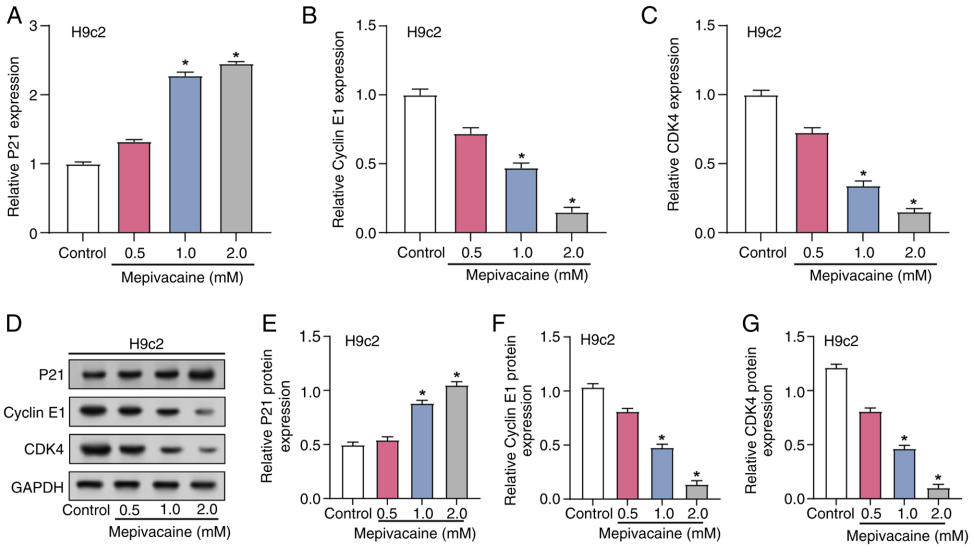

Figure 3. Impact of mepivacaine on the cell cycle of H9c2 cells. Evaluation of mRNA expression levels of cell cycle-related markers (A) P21, (B) Cyclin E1 and (C) CDK4 in H9c2 cells treated with different concentrations of mepivacaine using reverse transcription-quantitative PCR. (D) Representative western blotting images of protein expression levels of cell cycle-related markers (E) P21, (F) Cyclin E1 and (G) CDK4 in H9c2 cells treated with different concentrations of mepivacaine. Data are presented as mean ± SD. Statistical significance was assessed using one-way ANOVA followed by Tukey's post hoc test. *P<0.05 compared with the Control group.

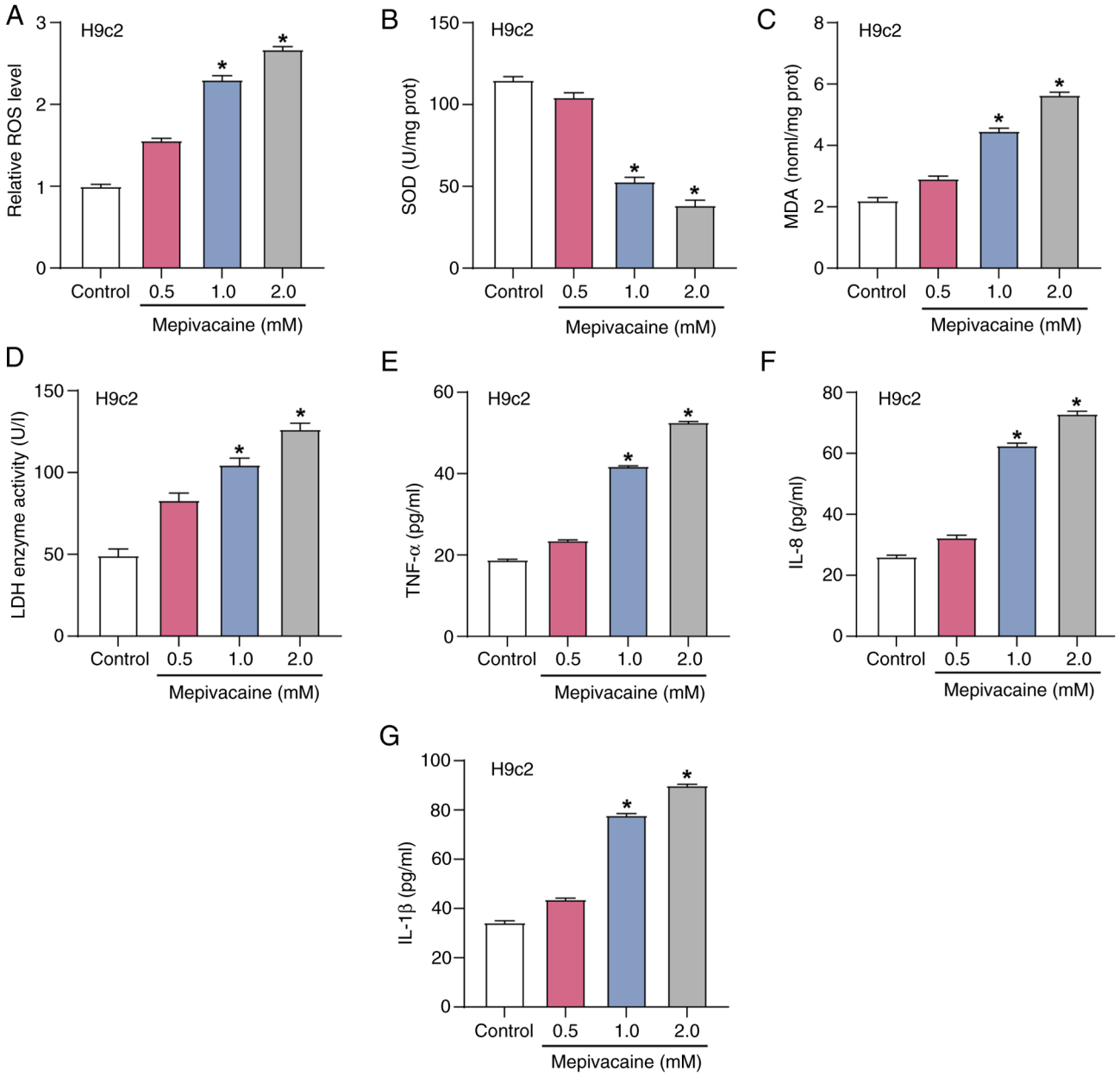

Figure 4. Mepivacaine induces oxidative stress and inflammation in H9c2 cells. Measurement of (A) ROS, (B) SOD, (C) MDA and (D) LDH levels in H9c2 cells treated with different concentrations of mepivacaine using corresponding assay kits. Assessment of the secretion levels of inflammatory cytokines (E) TNF-α, (F) IL-8 and (G) IL-1β in H9c2 cells treated with different concentrations of mepivacaine using ELISA. Data are presented as mean ± SD. Statistical significance was assessed using one-way ANOVA followed by Tukey's post hoc test. *P<0.05 compared with the Control group. ROS, reactive oxygen species; SOD, superoxide dismutase; MDA, malondialdehyde; LDH, lactate dehydrogenase; prot, protein.

to examine the impact of combined treatment with 2 mM mepivacaine and *CACNB1* knockdown on the levels of apoptotic proteins in H/R model H9c2 cells (Fig. 6B-F). Analysis revealed that, compared with the Control group, the expression of Caspase-3 and Bax was upregulated, whereas the expression of Bcl-2 was downregulated in the H/R group. However, upon additional *CACNB1* knockdown, the expression of Caspase-3 and Bax decreased, while the expression of Bcl-2 increased compared with the H/R group. These experiments demonstrated that *CACNB1* knockdown exerts anti-apoptotic effects, alleviating the damage induced by H/R and mepivacaine.

CACNB1 knockdown modulates the expression of inflammatory mediators and Nrf2 nuclear translocation in the H/R model treated with mepivacaine. WB analysis was employed to assess the impact of combined treatment with 2 mM mepivacaine and *CACNB1* knockdown on the levels of inflammatory-related factors (NLRP3, IL-1β, GSDMD, ASC, IL-18, Caspase-1 and C-Caspase-1) in H/R model H9c2 cells (Fig. 7A and B). Analysis revealed a noteworthy rise in the level of these inflammation-related factors in the H/R group, compared with the control group, while their expression was notably reduced in the H/R group with *CACNB1* knockdown compared with the H/R group. Previous research suggested that Nrf2 is involved in maintaining redox homeostasis and exhibits protective effects against MIRI (24). To investigate whether the anti-apoptotic effect induced by *CACNB1* knockdown is associated with Nrf2 nuclear translocation, the levels of nuclear

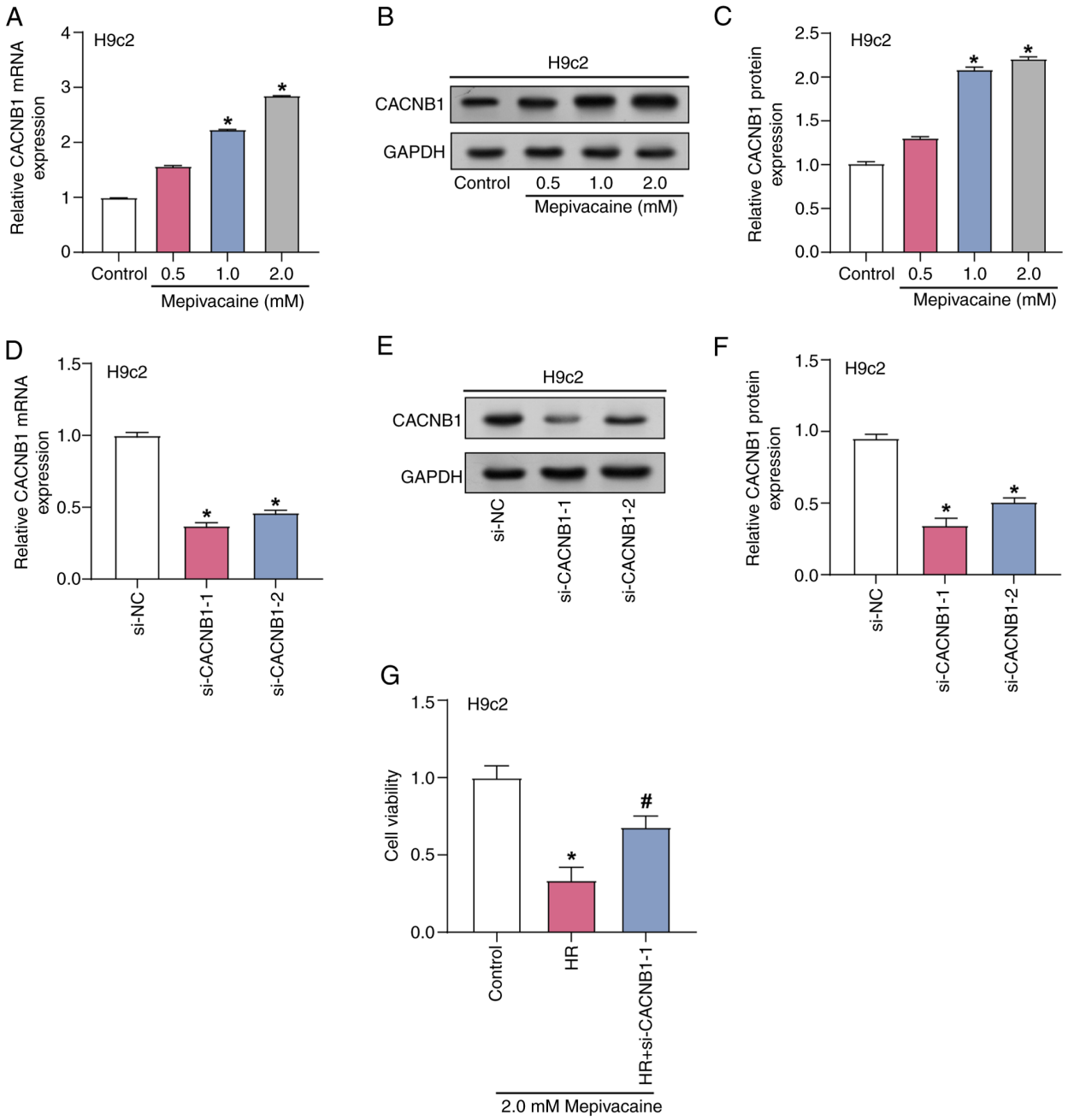

Figure 5. Impact of mepivacaine treatment and *CACNB1* knockdown on H9c2 cell viability. (A) mRNA expression levels (B) representative western blotting images and (C) protein expression levels of *CACNB1* in H9c2 cells treated with different concentrations of mepivacaine. (D) mRNA expression levels, (E) representative western blotting images and (F) protein expression levels of *CACNB1* to assess the transfection efficiency of *CACNB1* knockdown plasmids. (G) The viability of HR model H9c2 cells treated with 2 mM mepivacaine for 24 h, combined with *CACNB1* knockdown, was assessed using the Cell Counting Kit-8 assay. Data are presented as mean ± SD. Statistical significance was assessed using one-way ANOVA followed by Tukey's post hoc test. *P<0.05 compared with the Control group, $^{\#}$P<0.05 compared with the H/R group. HR, hypoxia/reoxygenation; si, small interfering.

Nrf2 and cytoplasmic Nrf2 proteins were assessed through WB analysis (Fig. 7C and D). Analysis revealed that compared with the Control group, the levels of cytoplasmic Nrf2 decreased, while the levels of nuclear Nrf2 increased in the H/R group. Furthermore, in the H/R group with CACNB1 knockdown, the level of nuclear Nrf2 increased and the level of cytoplasmic Nrf2 further decreased. These findings indicated that *CACNB1* knockdown advances the translocation of Nrf2 into the nucleus, indicating that *CACNB1* inhibits inflammation and apoptosis through the *CACNB1*/NLRP3/Nrf2 axis, thereby alleviating the damage induced by H/R and mepivacaine.

Discussion

MI, as a globally prevalent and highly lethal disease, has attracted considerable attention from clinicians and researchers. Zhao *et al* (25) identified genes such as *IL1R2*, *IRAK3* and *THBD* as diagnostic biomarkers for AMI, which are associated with immune cell infiltration. Scholars have summarized signaling pathways associated with MI, including inflammatory pathways such as TLR4/MyD88/NF-κB and NLRP3/Caspase-1, oxidative stress and apoptosis-related pathways such as Sonic hedgehog and Nrf2/HO-1 and key

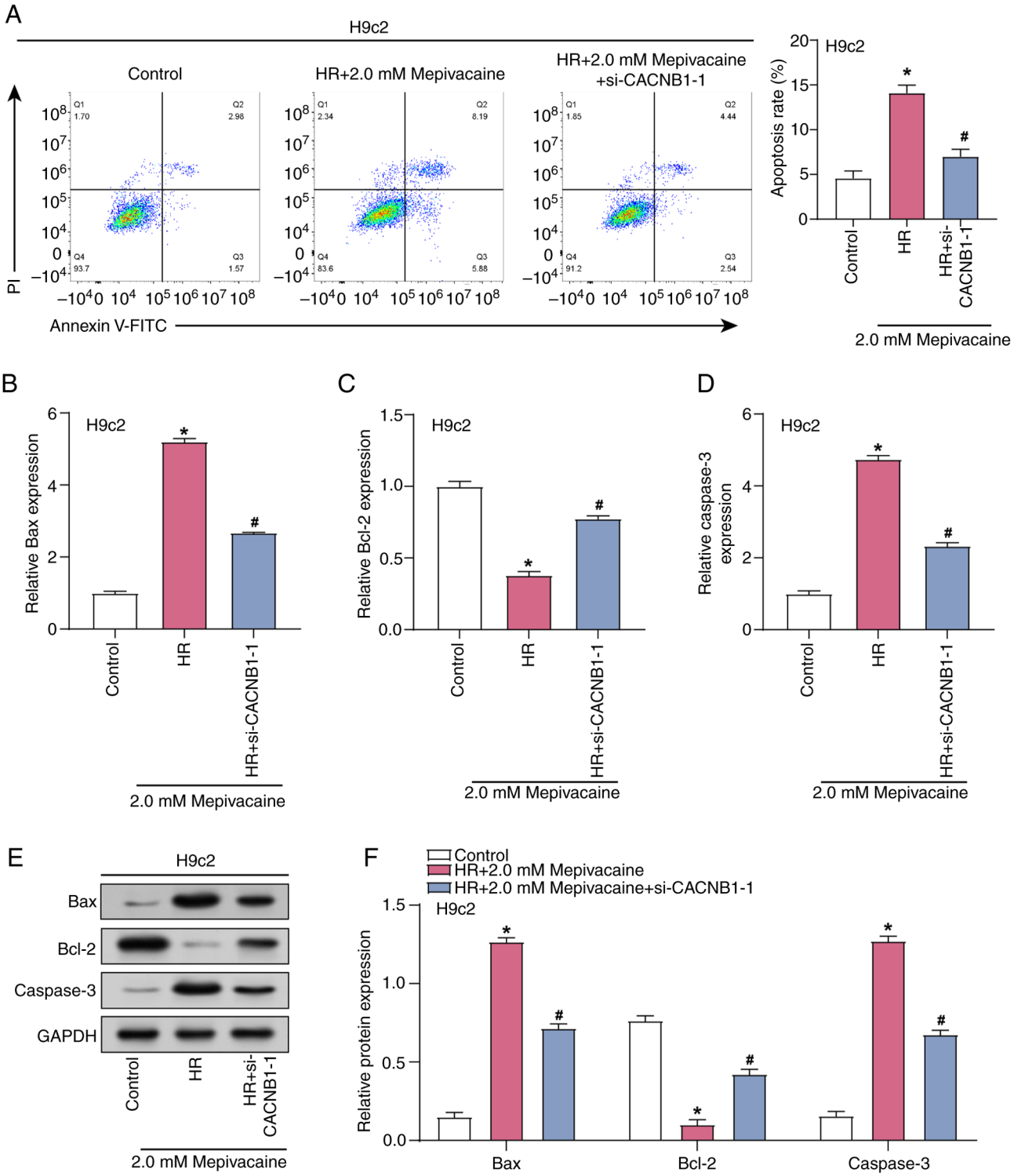

Figure 6. Effect of *CACNB1* knockdown on apoptosis in HR model H9c2 cells treated with mepivacaine. (A) Assessment of apoptosis level in HR model H9c2 cells treated with 2 mM mepivacaine and *CACNB1* knockdown using flow cytometry. Evaluation of the mRNA expression levels of apoptotic proteins (B) Bax, (C) Bcl-2 and (D) Caspase-3 in H/R model H9c2 cells treated with 2 mM mepivacaine and *CACNB1* knockdown. (E) Representative western blotting images and (F) protein expression of Bax, Bcl-1 and Caspase-1. Data are presented as mean ± SD. Statistical significance was assessed using one-way ANOVA followed by Tukey's post hoc test. *P<0.05 compared with the Control group, #P<0.05 compared with the H/R + 2.0 mM Mepivacaine group. HR, Hypoxia/Reoxygenation; si, small interfering.

regulators of angiogenesis such as PI3K/Akt and MAPK pathways, all carrying out key roles in the development of MI (26). The bioinformatic analysis of the present study, leveraging the GSE19339 dataset, supported these findings by identifying significant enrichment of 'Inflammatory Response' and 'PI3K-Akt signaling pathway' among the GSE19339-DEGs. Paolisso *et al* (27) revealed that patients with obstructive AMI with hyperglycaemia exhibited increased inflammation markers and larger infarct areas, whereas patients with non-obstructive AMI demonstrated less myocardial damage.

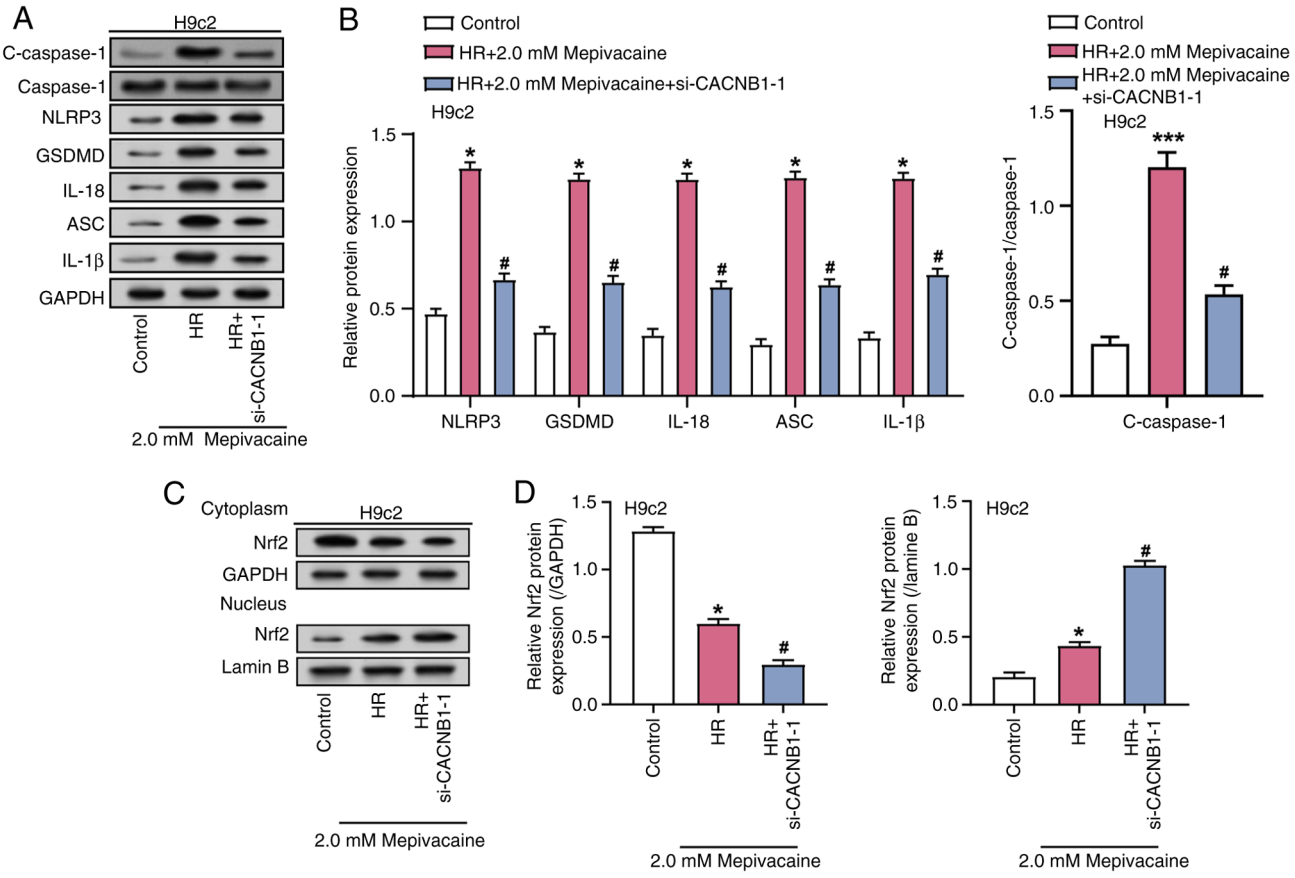

Figure 7. *CACNB1* knockdown modulates the expression of inflammatory mediators and Nrf2 nuclear translocation. (A) Representative western blotting images and (B) expression levels of inflammatory-related factors (NLRP3, C-Caspase-1, GSDMD, IL-18, ASC and IL-1β) were evaluated by western blot analysis upon combined treatment with mepivacaine and *CACNB1* knockdown. (C) Representative western blotting images and (D) expression levels of cytoplasmic Nrf2 and nuclear Nrf2 proteins were assessed by western blot analysis. Data are presented as mean ± SD. Statistical significance was assessed using one-way ANOVA followed by Tukey's post hoc test. *P<0.05 and ***P<0.001 compared with the Control group, $^{\#}$P<0.05 compared with the H/R + 2.0 mM Mepivacaine group. HR, Hypoxia/Reoxygenation; si, small interfering; Nrf2, nuclear factor erythroid 2-related factor 2; ASC, apoptosis-associated speck-like protein containing a CARD (also known as PYCARD).

Additionally, the hypothesis by Zhao *et al* (28) that the long non-coding RNA MI Associated Transcript regulates the PI3K/Akt pathway, which potentially influences myocardial fibrosis and heart failure, underscores the complexity of post-MI remodeling processes. Notably, the findings of the present study also revealed an upregulation of CACNB1 in MI samples, indicating its pivotal role in cardiac dysfunction and the progression of disease pathology. This positions *CACNB1* as a potential target for therapeutic intervention, aiming to modulate cardiac responses to ischemic stress and improve outcomes in patients with MI.

Mepivacaine, an amide-type local anesthetic known for its rapid diffusion and brief duration, is widely used in surgery and dentistry (29,30). While essential for effective pain management, its potential for cardiac toxicity requires careful use, especially in patients with cardiovascular risks (31). The current research on H9c2 cardiomyocytes revealed that mepivacaine may exacerbate myocardial injury, characterized by notable cell cycle arrest and activation of apoptosis. This effect is characterized by a reduction in the anti-apoptotic Bcl-2 and increases in the pro-apoptotic markers Caspase-3 and Bax, suggesting that mepivacaine could intensify cell death pathways that are important under ischemic conditions. Furthermore, mepivacaine treatment disrupted cell cycle progression by inducing a G_1 phase arrest, as demonstrated by increased P21 expression and decreased levels of Cyclin E1 and CDK4. Importantly, mepivacaine elevates oxidative stress markers such as ROS and MDA, indicators of increased oxidative damage (32). Oxidative stress is a major factor in cellular damage during MI, where it contributes to cell membrane damage through mechanisms such as lipid peroxidation, evidenced by elevated MDA levels. This oxidative damage is particularly key during IR events, characterized by a rapid increase in oxygen that leads to excessive ROS production. This surge can overwhelm the antioxidant defenses of a cell, such as SOD, which was observed to be diminished in the present study. This imbalance between pro-oxidants and antioxidants exacerbates cellular injury, underscoring the deleterious impact of mepivacaine on myocardial health, especially under ischemic conditions. Inflammation is another key factor in the pathophysiology of MI, with cytokines such as IL-1β, IL-8 and TNF-α carrying out key roles in mediating inflammatory responses (33,34). These cytokines are known to influence the infarct size and intensity of myocardial injury by promoting further inflammatory cell infiltration and activating additional cytotoxic pathways (35). The present study revealed that mepivacaine elevates these cytokines, potentially increasing the inflammatory response in myocardial tissues,

which could exacerbate the damage in ischemic conditions. These findings highlight the ability of mepivacaine to amplify cardiomyocyte oxidative stress and inflammatory responses.

As an integral component of calcium ion channels, *CACNB1* carries out a key role in regulating calcium ion permeability across cell membranes and maintaining intracellular calcium levels (36). In the present study, CACNB1 expression increased as mepivacaine concentration increased, suggesting its involvement in the cellular response to mepivacaine exposure. MIRI is a considerable pathophysiological component of MI, where, despite the restoration of blood supply alleviating ischemia, reperfusion itself can induce further myocardial damage (37). Reperfusion is known to trigger inflammatory responses, activate inflammatory cells and release mediators that exacerbate myocardial damage and remodeling (38). A recent study by Algoet *et al* (39) emphasized the intertwined mechanisms of IR injury and inflammatory changes and explored dual intervention strategies as potential therapeutic approaches. It is well-documented that MIRI can lead to calcium overload (40-42), worsening MIRI. Specifically, myocardial cell-specific loss of the NBCe1 Na^+-HCO^{3-} cotransporter was revealed to confer cardioprotective effects during IR injury (43). Additionally, disruptions in Ca^{2+} homeostasis, commonly observed in cardiac IR and heart failure, were associated with mitochondrial-associated membrane between the endoplasmic reticulum and mitochondria, affecting Ca^{2+} transport and suggesting new therapeutic targets for cardiac diseases (44,45). In the present study, experiments using the H/R model demonstrated that knocking down *CACNB1* could alleviate cell damage induced by H/R and mepivacaine, providing novel insights into myocardial cell protection mechanisms. These results emphasize the importance of understanding the role of *CACNB1* in calcium regulation and its potential as a focus to lessen myocardial injury in the setting of IR.

NLRP3 and Nrf2 represent two key regulatory pathways involved in inflammation and oxidative stress responses (46,47). The multi-protein complex known as the NLRP3 inflammasome is primarily produced by immunological cells, including dendritic and macrophage cells (48). Conversely, Nrf2 acts as a major regulator of cellular antioxidant defense mechanisms. Emerging evidence suggests a complex interplay between the NLRP3 inflammasome and the Nrf2 pathway (49). While triggering the NLRP3 inflammasome promotes inflammation and oxidative stress, activation of Nrf2 exerts anti-inflammatory and antioxidative effects. Nie *et al* (50) revealed that the SIRT1/NRF2 signaling pathway is the true target of resveratrol and carries out a key part in the cardioprotective effect against inflammation induced by resveratrol. Mauro *et al* (51) highlighted that NLRP3 senses intracellular danger signals during ischemia and extracellular or intracellular alarm molecules during tissue injury and highlighted its role in initiating inflammation and cell death through activation of caspase-1. Shen *et al* (52) further emphasized the role of Nrf2 in maintaining redox balance and demonstrated that the Nrf2/Keap1/ARE pathway is key in reducing the size of MI and protecting the cardiac function after MIRI.

In line with these insights, the present study investigated the effects of CACNB1 knockdown in an H/R model treated with mepivacaine. WB analysis revealed that CACNB1 knockdown modulates inflammatory mediators, such as NLRP3 and IL-1β, and notably promotes Nrf2 translocation into the nucleus. This suggested a protective mechanism against H/R-induced myocardial injury, where *CACNB1* knockdown not only reduces inflammatory and apoptotic signaling but also enhances the antioxidant response. The decreased expression of cytoplasmic Nrf2 and increased Nrf2 translocation to the nucleus in the H/R model with *CACNB1* knockdown demonstrated a dynamic shift towards enhancing cellular resilience against oxidative stress. These findings highlight the CACNB1/NLRP3/Nrf2 axis as a strategic approach to alleviate inflammation and enhance antioxidant defenses, offering potential therapeutic pathways to reduce myocardial injury during IR, particularly in treatments involving mepivacaine and other stressors.

The use of the H9c2 cell line in the present study provided a valuable model for investigating the effects of mepivacaine on cardiomyocytes. However, it is essential to acknowledge the potential limitations associated with using a single cell line rather than primary cardiomyocytes. H9c2 cells, derived from embryonic rat heart tissue, may not fully recapitulate the mature phenotype and complex physiological responses of adult cardiomyocytes. Additionally, the genetic homogeneity of the cell line may limit the generalizability of the current findings to a broader population. While H9c2 cells offer reproducibility and ease of use, their response to experimental conditions may differ from that of primary cardiomyocytes, which are embedded in a native extracellular matrix and exhibit more diverse genetic backgrounds. Future studies should aim to validate these findings in primary cardiomyocytes or *in vivo* models to further elucidate the physiological relevance of present observations.

In conclusion, the present study elucidated the potential cardiotoxic effects of mepivacaine, particularly in the context of MIRI. *CACNB1* was identified as a key player in mediating mepivacaine-induced cardiomyocyte injury and demonstrated its involvement in apoptosis and inflammation pathways. Through *CACNB1* knockdown, a notable protection against mepivacaine and H/R-induced damage was observed, evidenced by improved cell viability, reduced apoptosis and modulation of inflammatory mediators. Importantly, the current findings revealed a novel mechanism involving the *CACNB1*/NLRP3/Nrf2 axis, wherein *CACNB1* knockdown facilitates Nrf2 nuclear translocation, thereby mitigating inflammation and apoptosis in cardiomyocytes. These insights shed light on potential therapeutic targets for mitigating mepivacaine-induced cardiotoxicity and offer novel perspectives for the development of cardioprotective strategies, particularly within the framework of perioperative cardiac care. Further investigation into the precise molecular mechanisms underlying *CACNB1*-mediated cardioprotection is warranted to fully harness its therapeutic potential in clinical settings.

Acknowledgements

Not applicable.

Funding

No funding was received.

Availability of data and materials

The data generated in the present study may be requested from the corresponding author.

Authors' contributions

QS, JZ and HW contributed to the conception and design of the present study. QS and JZ contributed to acquisition of data. QS and JZ contributed to analysis and interpretation of data. QS contributed to statistical analysis. QS and JZ contributed to drafting the manuscript. HW contributed to revision of manuscript for important intellectual content. QS and HW confirm the authenticity of all the raw data. All the authors read and approved the final manuscript.

Ethics approval and consent to participate

Not applicable.

Patient consent for publication

Not applicable.

Competing interests

The authors declare that they have no competing interests.

References

1. Katari V, Kanajam LSP, Kokkiligadda S, Sharon T and Kantamaneni P: A review on causes of myocardial infarction and its management. World J Pharmaceutical Res 12: 511-529, 2023.
2. Sagris M, Antonopoulos AS, Theofilis P, Oikonomou E, Siasos G, Tsalamandris S, Antoniades C, Brilakis ES, Kaski JC and Tousoulis D: Risk factors profile of young and older patients with myocardial infarction. Cardiovasc Res 118: 2281-2292, 2022.
3. Khan IA, Karim HMR, Panda CK, Ahmed G and Nayak S: Atypical presentations of myocardial infarction: A systematic review of case reports. Cureus 15: e35492, 2023.
4. Camacho X, Nedkoff L, Wright FL, Nghiem N, Buajitti E, Goldacre R, Rosella LC, Seminog O, Tan EJ, Hayes A, *et al*: Relative contribution of trends in myocardial infarction event rates and case fatality to declines in mortality: An international comparative study of 1 95 million events in 80 4 million people in four countries. Lancet Public Health 7: e229-e239, 2022.
5. Fathima SN: An update on myocardial infarction. Curr Res Trends Med Sci Technol 1: 15, 2021.
6. Dos Santos CC, Matharoo AS, Cueva EP, Amin U, Ramos AAP, Mann NK, Maheen S, Butchireddy J, Falki VB, Itrat A, *et al*: The influence of sex, age, and race on coronary artery disease: A narrative review. Cureus 15: e47799, 2023.
7. Radu RI, Ben Gal T, Abdelhamid M, Antohi EL, Adamo M, Ambrosy AP, Geavlete O, Lopatin Y, Lyon A, Miro O, *et al*: Antithrombotic and anticoagulation therapies in cardiogenic shock: A critical review of the published literature. ESC Heart Fail 8: 4717-4736, 2021.
8. Zangrillo A, Lomivorotov VV, Pasyuga VV, Belletti A, Gazivoda G, Monaco F, Nigro Neto C, Likhvantsev VV, Bradic N, Lozovskiy A, *et al*: Effect of volatile anesthetics on myocardial infarction after coronary artery surgery: A post hoc analysis of a randomized trial. J Cardiothorac Vasc Anesth 36: 2454-2462, 2022.
9. Körner J, Albani S, Sudha Bhagavath Eswaran V, Roehl AB, Rossetti G and Lampert A: Sodium channels and local anesthetics-old friends with new perspectives. Front Pharmacol 13: 837088, 2022.
10. Gitman M, Fettiplace MR, Weinberg GL, Neal JM and Barrington MJ: Local anesthetic systemic toxicity: A narrative literature review and clinical update on prevention, diagnosis, and management. Plast Reconstr Surg 144: 783-795, 2019.
11. Dell'Olio F, Capodiferro S, Lorusso P, Limongelli L, Tempesta A, Massaro M, Grasso S and Favia G: Light conscious sedation in patients with previous acute myocardial infarction needing exodontia: An observational study. Cureus 11: e6508, 2019.
12. Mosqueira M, Aykut G and Fink RH: Mepivacaine reduces calcium transients in isolated murine ventricular cardiomyocytes. BMC Anesthesiol 20: 10, 2020.
13. de Groot-van der Mooren M, Quint S, Knobbe I, Cronie D and van Weissenbruch M: Severe cardiorespiratory and neurologic symptoms in a neonate due to mepivacaine intoxication. Case Rep Pediatr 2019: 4013564, 2019.
14. Andrade A, Brennecke A, Mallat S, Brown J, Gomez-Rivadeneira J, Czepiel N and Londrigan L: Genetic associations between voltage-gated calcium channels and psychiatric disorders. Int J Mol Sci 20: 3537, 2019.
15. Gilbert G, Demydenko K, Dries E, Puertas RD, Jin X, Sipido K and Roderick HL: Calcium signaling in cardiomyocyte function. Cold Spring Harb Perspect Biol 12: a035428, 2020.
16. Shah K, Seeley S, Schulz C, Fisher J and Gururaja Rao S: Calcium channels in the heart: Disease states and drugs. Cells 11: 943, 2022.
17. Erdogmus S, Concepcion AR, Yamashita M, Sidhu I, Tao AY, Li W, Rocha PP, Huang B, Garippa R, Lee B, *et al*: Cavβ1 regulates T cell expansion and apoptosis independently of voltage-gated Ca2+ channel function. Nat Commun 13: 2033, 2022.
18. Xuan L, Zhu Y, Liu Y, Yang H, Wang S, Li Q, Yang C, Jiao L, Zhang Y, Yang B and Sun L: Up-regulation of miR-195 contributes to cardiac hypertrophy-induced arrhythmia by targeting calcium and potassium channels. J Cell Mol Med 24: 7991-8005, 2020.
19. Livak KJ and Schmittgen TD: Analysis of relative gene expression data using real-time quantitative PCR and the 2(-Delta Delta C(T)) method. Methods 25: 402-408, 2001.
20. Lu Y, Zhang Y, Wang N, Pan Z, Gao X, Zhang F, Zhang Y, Shan H, Luo X, Bai Y, *et al*: MicroRNA-328 contributes to adverse electrical remodeling in atrial fibrillation. Circulation 122: 2378-2387, 2010.
21. Couch LS, Fiedler J, Chick G, Clayton R, Dries E, Wienecke LM, Fu L, Fourre J, Pandey P, Derda AA, *et al*: Circulating microRNAs predispose to takotsubo syndrome following high-dose adrenaline exposure. Cardiovasc Res 118: 1758-1770, 2022.
22. Scarparo HC, Maia RN, Filho ED, Soares E, Costa F, Fonteles C, Bezerra TP, Ribeiro TR and Romero NR: Plasma mepivacaine concentrations in patients undergoing third molar surgery. Aust Dent J 61: 446-454, 2016.
23. Zhou Q and Zhang L: MicroRNA-183-5p protects human derived cell line SH-SY5Y cells from mepivacaine-induced injury. Bioengineered 12: 3177-3187, 2021.
24. Cheng L, Zhang H, Wu F, Liu Z, Cheng Y and Wang C: Role of Nrf2 and its activators in cardiocerebral vascular disease. Oxid Med Cell Longev 2020: 4683943, 2020.
25. Zhao E, Xie H and Zhang Y: Predicting diagnostic gene biomarkers associated with immune infiltration in patients with acute myocardial infarction. Front Cardiovasc Med 7: 586871, 2020.
26. Zhang Q, Wang L, Wang S, Cheng H, Xu L, Pei G, Wang Y, Fu C, Jiang Y, He C and Wei Q: Signaling pathways and targeted therapy for myocardial infarction. Signal Transduct Target Ther 7: 78, 2022.
27. Paolisso P, Foà A, Bergamaschi L, Donati F, Fabrizio M, Chiti C, Angeli F, Toniolo S, Stefanizzi A, Armillotta M, *et al*: Hyperglycemia, inflammatory response and infarct size in obstructive acute myocardial infarction and MINOCA. Cardiovasc Diabetol 20: 33, 2021.
28. Zhao X, Ren Y, Ren H, Wu Y, Liu X, Chen H and Ying C: The mechanism of myocardial fibrosis is ameliorated by myocardial infarction-associated transcript through the PI3K/Akt signaling pathway to relieve heart failure. J Int Med Res: Jul 18, 2021.
29. Burgos EG, García-García LL, Gómez-Serranillos MP and Oliver FG: Local Anesthetics. Adv Neuropharmacol: 351-388, 2020.
30. Lottinger C: Local anesthetics in dentistry. In: Evidence-Based Oral Surgery. Springer, London, pp129-150, 2019.
31. Ozbay S, Ayan M and Karcioglu O: Local anesthetics, clinical uses, and toxicity: Recognition and management. Curr Pharm Des 29: 1414-1420, 2023.
32. Aladağ N, Asoğlu R, Ozdemir M, Asoğlu E, Derin AR, Demir C and Demir H: Oxidants and antioxidants in myocardial infarction (MI): Investigation of ischemia modified albumin, malondialdehyde, superoxide dismutase and catalase in individuals diagnosed with ST elevated myocardial infarction (STEMI) and non-STEMI (NSTEMI). J Med Biochem 40: 286, 2021.

33. Mitsis A, Kadoglou NP, Lambadiari V, Alexiou S, Theodoropoulos KC, Avraamides P and Kassimis G: Prognostic role of inflammatory cytokines and novel adipokines in acute myocardial infarction: An updated and comprehensive review. Cytokine 153: 155848, 2022.
34. Zhang H and Dhalla NS: The role of pro-inflammatory cytokines in the Pathogenesis of Cardiovascular Disease. Int J Mol Sci 25: 1082, 2024.
35. Shao L, Shen Y, Ren C, Kobayashi S, Asahara T and Yang J: Inflammation in myocardial infarction: Roles of mesenchymal stem cells and their secretome. Cell Death Discov 8: 452, 2022.
36. Tuluc P, Theiner T, Jacobo-Piqueras N and Geisler SM: Role of high Voltage-Gated Ca2+ Channel subunits in pancreatic β-cell insulin release. From structure to function. Cells 10: 2004, 2021.
37. Zhang S, Yan F, Luan F, Chai Y, Li N, Wang YW, Chen ZL, Xu DQ and Tang YP: The pathological mechanisms and potential therapeutic drugs for myocardial ischemia reperfusion injury. Phytomedicine 129: 155649, 2024.
38. Zhang D, Wu H, Liu D, Li Y and Zhou G: Research progress on the mechanism and treatment of inflammatory response in myocardial Ischemia-reperfusion injury. Heart Surg Forum 25: E462-E468, 2022.
39. Algoet M, Janssens S, Himmelreich U, Gsell W, Pusovnik M, Van den Eynde J and Oosterlinck W: Myocardial ischemia-reperfusion injury and the influence of inflammation. Trends Cardiovasc Med 33: 357-366, 2023.
40. Li YW, Liu Y, Luo SZ, Huang XJ, Shen Y, Wang WS and Lang ZC: The significance of calcium ions in cerebral ischemia-reperfusion injury: Mechanisms and intervention strategies. Front Mol Biosci 12: 1585758, 2025.
41. He J, Liu D, Zhao L, Zhou D, Rong J, Zhang L and Xia Z: Myocardial ischemia/reperfusion injury: Mechanisms of injury and implications for management. Exp Ther Med 23: 430, 2022.
42. Trujillo-Rangel WÁ, García-Valdés L, Méndez-del Villar M, Castañeda-Arellano R, Totsuka-Sutto SE and García-Benavides L: Therapeutic targets for regulating oxidative damage induced by ischemia-reperfusion injury: A study from a pharmacological perspective. Oxid Med Cell Longev 2022: 8624318, 2022.
43. Vairamani K, Prasad V, Wang Y, Huang W, Chen Y, Medvedovic M and Lorenz JN and Shull GE: NBCe1 Na+-HCO3-cotransporter ablation causes reduced apoptosis following cardiac ischemia-reperfusion injury in vivo. World J Cardiol 10: 97, 2018.
44. Wang Y, Zhang X, Wen Y, Li S, Lu X, Xu R and Li C: Endoplasmic reticulum-mitochondria contacts: A potential therapy target for cardiovascular remodeling-associated diseases. Front Cell Dev Biol 9: 774989, 2021.
45. Luan Y, Luan Y, Yuan R-X, Feng Q, Chen X and Yang Y: Structure and function of mitochondria-associated endoplasmic reticulum membranes (MAMs) and their role in cardiovascular diseases. Oxid Med Cell Longev 2021: 4578809, 2021.
46. Li W, Cao T, Luo C, Cai J, Zhou X, Xiao X and Liu S: Crosstalk between ER stress, NLRP3 inflammasome, and inflammation. Appl Microbiol Biotechnol 104: 6129-6140, 2020.
47. Saha S, Buttari B, Panieri E, Profumo E and Saso L: An overview of Nrf2 signaling pathway and its role in inflammation. Molecules 25: 5474, 2020.
48. Wang L and Hauenstein AV: The NLRP3 inflammasome: Mechanism of action, role in disease and therapies. Mol Aspects Med 76: 100889, 2020.
49. Tastan B, Arioz BI and Genc S: Targeting NLRP3 inflammasome with Nrf2 inducers in central nervous system disorders. Front Immunol 13: 865772, 2022.
50. Nie Q, Zhang J, He B, Wang F, Sun M, Wang C, Sun W, Guo J, Wen J and Liu P: A novel mechanism of protection against isoproterenol-induced cardiac inflammation via regulation of the SIRT1/NRF2 signaling pathway with a natural SIRT1 agonist. Eur J Pharmacol 886: 173398, 2020.
51. Mauro AG, Bonaventura A, Mezzaroma E, Quader M and Toldo S: NLRP3 inflammasome in acute myocardial infarction. J Cardiovasc Pharmacol 74: 175-187, 2019.
52. Shen Y, Liu X, Shi J and Wu X: Involvement of Nrf2 in myocardial ischemia and reperfusion injury. Int J Biol Macromol 125: 496-502, 2019.